Applied Materials Today 15 (2019) 288–289

Contents lists available at ScienceDirect

Applied Materials Today

journal homepage: www.elsevier.com/locate/apmt

Exploring quantification in a mixture using graphene-based surface-enhanced Raman spectroscopy

Huihui Tian[a,b], Na Zhang[a], Jin Zhang[a], Lianming Tong[a,*]

[a] Center for Nanochemistry, State Key Laboratory for Structural Chemistry of Unstable and Stable Species, Beijing National Laboratory for Molecular Sciences, College of Chemistry and Molecular Engineering, Peking University, Beijing 100871, China
[b] CAS Key Laboratory for Biomedical Effects of Nanomaterials and Nanosafety, CAS Center for Excellence in Nanoscience, National Center for Nanoscience and Technology, Beijing 100190, China

ARTICLE INFO

Article history:
Received 25 December 2018
Accepted 22 January 2019

Keywords:
Graphene
Surface-enhanced Raman scattering
Quantitative analysis
Internal standard
Complex system

ABSTRACT

Quantitative analysis is a demanding challenge for surface-enhanced Raman scattering (SERS). A number of methods have been developed using different SERS-active substrates for quantitative detection of certain species. However, for a target analyte that is mixed with other molecules, the competitive adsorption of other molecules on the SERS substrate becomes the major disturbance to quantitative analysis or even qualitative detection. Whether it is possible to quantitatively detect a single analyte in a mixture of molecules using SERS has remained unclear. In this work, we explored the possibility of quantitative detection of multiple analytes by using graphene-based SERS (G-SERS). Graphene provides an atomically flat surface for homogeneous adsorption of molecules, and its own Raman scattering intensity can serve as internal standard in SERS for quantitative analysis. Our results show that the adsorption constants, the concentration and the Raman scattering cross sections of competing species are the most important factors to be considered. The findings could be helpful for quantitative analysis of target analyte in practical complex systems.

1. Introduction

Surface-enhanced Raman spectroscopy (SERS) is a powerful and sensitive technique for the detection of fingerprint signal of molecules and the investigation of a series of surface chemical reactions [1–4]. The "hot spots" in a SERS substrate can provide high enhancement factors ($EF \geq 10^7$) so that the detection of single molecules has been possible [5–8]. As a result, SERS has played an important role in various applications from food safety, medical diagnostics to environmental monitoring [9–12].

Quantitative analysis has been one of the most important and challenging applications of SERS [13]. So far a few approaches have been developed for quantitative SERS detection of single species [6,12–16]. Shen et al. developed a kind of core-molecule-shell nanoparticle (CMS NP), which has a framework molecule to form the shell between Au core and Ag shell layer and a probe molecule as a Raman internal standard, to realize the quantitative analysis of target molecules that adhere on the nanoparticles [14]. Chen et al. used alkanethiolate ligand-capped Ag nanoparticle film to realize the quantitative SERS measurement down to single-molecules level [6]. However, for practical applications, there are inevitably other molecules coexisting with the target molecule, which competes in adsorption on the active sites of the SERS substrate and interference the quantification. Thus the quantification in multiple mixtures of analytes requires the consideration of the chemical and physical interactions between the substrate and different species in a liquid [17–19] and the development of the analytical models [20,21]. Specific interaction with a target molecule is a feasible approach [22–25], e.g. Qiao et al. prepared a kind of SERS sensor based on the self-assembly of gold superparticles on metal organic framework, which can specifically detect gaseous aldehydes that are released as a result of tumor-specific tissue composition and metabolism, therefore realized the indicators of lung cancer [24]. Lu et al. developed a kind of Hg^{2+} sensor based on the formation of T–Hg^{2+}–T pairs and the corresponding orientation variation of DNA on Au shell surface [25]. However, for labeled SERS substrates, it is still possible that molecules with similar structure as the target analyte preferentially adsorb on the active sites. In order to identify the fingerprint signal of the target analyte in a mixture, one needs the profound understanding of the adsorption behaviors and Raman scattering feature of each component in the mixture.

* Corresponding author.
E-mail address: tonglm@pku.edu.cn (L. Tong).

https://doi.org/10.1016/j.apmt.2019.01.008
2352-9407/

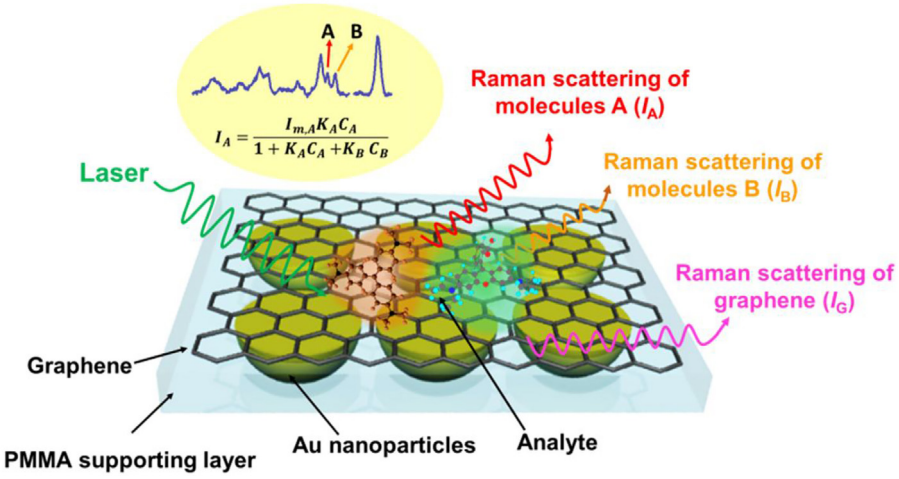

Fig. 1. Scheme of using G-SERS substrate to detect a binary system.

In this work, we employ graphene-based SERS (G-SERS) to analyze quantitative SERS for multiple components. As schematically shown in Fig. 1, graphene provides an atomically flat surface for homogeneous adsorption of molecules, which simplifies the model for quantitative analysis, particularly for the analysis of multiple components. Graphene also plays a role as the internal standard (IS) material that can be used to calibrate the fluctuation of Raman intensities of molecules due to the inhomogeneous distribution of hotspots on the SERS substrate and the variation of experimental parameters [26–29]. The latter is crucial in practical quantitative applications, where the laser power and spot size differ in different measurements.

Crystal violet (CV), rhodamine B (RhB) and rhodamine 6G (R6G) were chosen as probe molecules during quantitative G-SERS measurements following our previous work [27]. We studied the quantitative detection of one molecule with the existence of another. It was found that the adsorption of molecules on the surface of graphene follows the model of Langmuir adsorption isotherm. Due to the competitive adsorption of RhB or R6G molecules on the surface of graphene, the detected concentration of CV molecules deviated significantly depending on the concentration and Raman scattering cross section of RhB or R6G molecules. The correction of the standard curve of CV was proposed by considering the adsorption constant (K_T) and the concentration (C) of the interfering component. As a result, the quantitative detection of a target molecule in a mixture requires the knowledge of the adsorption constant, the concentration and the Raman scattering cross sections of the competing species. However, in practical applications, these parameters are typically unknown for the competing components. Nevertheless, our results can be useful in understanding the adsorption kinetics in complex solutions and be of help in further development of multiplex quantitative analysis based on SERS.

2. Experiment

2.1. Materials and equipment

Crystal violet (CV, >90%) was purchased from Sigma Aldrich; rhodamine B (RhB, 99%) and rhodamine 6G (R6G, 99%) were from Alfa Aesar (China). Raman measurements were carried out using a Horiba-Jobin Yvon system with a 633 nm He–Ne laser line. A 50× objective was used to focus the laser and the power on the sample was 1.0 mW.

2.2. SERS measurements

The transparent G-SERS substrates were prepared on PMMA polymer according to our previous work [26,30]. The SERS measurements were carried out by floating the G-SERS substrate on the surface of CV and RhB (or R6G) aqueous solution with graphene in contact with the solution [27]. The excitation laser was focused on graphene through the transparent PMMA polymer. All SERS spectra were collected until the adsorption of molecules reached equilibrium, which took ~10 min.

3. Results and discussion

In order to study the co-adsorption of multiple species, we first studied the adsorption and desorption behaviors of CV and RhB molecules. The normalized peak intensities ($I_R = I_{molecule}/I_{G\_2D}$) of CV (1621 cm^{-1}, blue area) and RhB (1650 cm^{-1}, red area) to that of graphene (2650 cm^{-1}) were monitored. These two modes were chosen because they are assigned to in-plane vibrations that may experience the same electromagnetic enhancement as graphene due to the excitation of surface plasmons in the gold film. Previous reports showed that the binding constants (K_T) of CV on the surface of graphene is 3.35×10^6 M^{-1}, which is ~3 times higher than that of RhB molecules 1.37×10^6 M^{-1}) [27]. This indicates that CV can be a stronger competing species than RhB molecules in adsorption on graphene. Fig. 1a and c shows the temporal Raman spectra and relative intensities (I_R) of RhB and CV during an exchange process, respectively. The G-SERS substrate was first placed on the surface of 5×10^{-6} M RhB solution for 10 min for saturated adsorption, and then put onto the surface of 5×10^{-6} M CV solution. We can see that the Raman signal of RhB decreased rapidly and disappeared in 5 min, while the signal of CV molecules increased significantly. For comparison, the desorption of RhB on graphene in deionized water was also measured, as shown in Fig. S1. It was found that the Raman signal of RhB deceased much slower in deionized water. After 100 min, the relative intensity remained at ~0.04. The fitted desorption constant of RhB in CV solution is ~9 times of that in distilled water (Fig. S1c). This confirmed that the competitive adsorption of CV molecules significantly accelerated the desorption of RhB from graphene. In Fig. 1b and d, the temporal Raman spectra and relative intensities of CV during desorption in the presence of RhB are shown. The initial concentration of CV and RhB were all 5×10^{-6} M. It is seen that the decrease of Raman intensity of CV was much slower. After 2 h, the relative intensity of CV

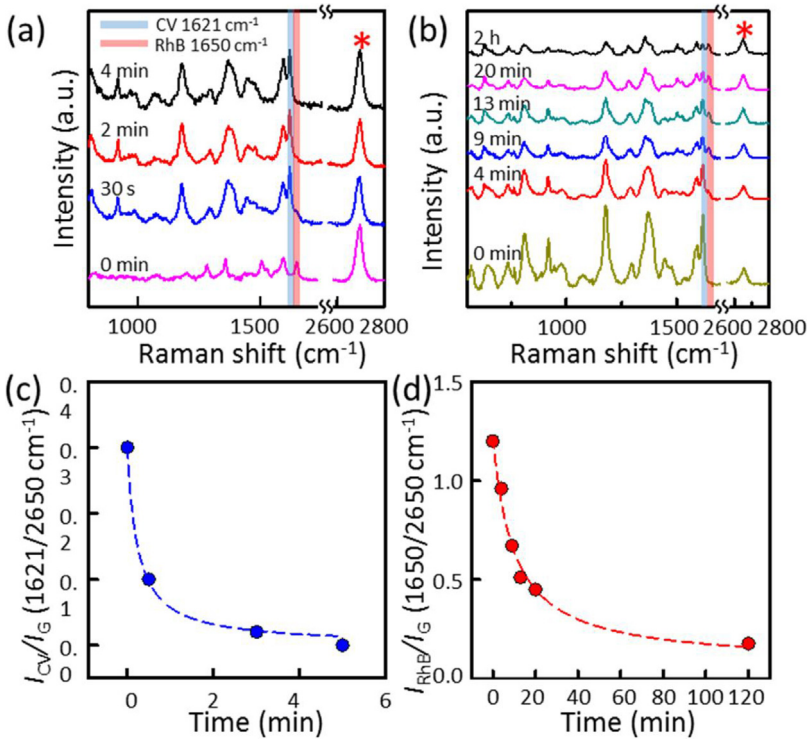

Fig. 2. The exchange behaviors of CV and RhB with each other on G-SERS substrate: (a) the G-SERS substrate was put on RhB solution first and then on CV solution and (b) the G-SERS substrate was put on CV solution first and then on RhB solution; (c and d) the in situ detection of relative Raman intensity I_R for (a) and (b) process respectively.

still remained at 0.2 owing to its much larger binding constant on grapheme (Fig. 2).

The competitive adsorption of CV and RhB on G-SERS substrate was further studied using aqueous solutions with these two molecules. The total concentration was fixed at of 5×10^{-6} M with the molar fraction of CV (χ_{CV}) varying from 0.0 to 1.0. The G-SERS substrate was then placed on the surface of the solution. SERS spectra were measured after ~10 min when the adsorption of molecules was saturated. Fig. 3a shows a series of representative Raman spectra of the mixture with different fractions of CV. The relative intensities (I_R) of CV (1621 cm^{-1}) and RhB (1650 cm^{-1}) to the 2D peak of graphene were plotted in Fig. 3b as a function of the fraction of CV.

The Langmuir isothermal model for multiple adsorbents has been developed by Butler and Ockrent et al., which assumed homogeneous adsorption and no interaction between adsorbed species [31,32]. The coverage of molecules on surface (θ) was denoted as the number ratio of the adsorbed molecules to the maximum number of adsorbed molecules covered in two-dimensional densely stacking per unit. According to this model, the surface coverage and the corresponding Raman intensity for CV molecules on graphene surface are as follows:

$$\theta_{CV} = \frac{K_{CV} \cdot C_{CV}}{1 + K_{CV} \cdot C_{CV} + K_{RhB} \cdot C_{RhB}} \quad (1)$$

and

$$I_{CV} = \frac{I_{m,CV} \cdot K_{CV} \cdot C_{CV}}{1 + K_{CV} \cdot C_{CV} + K_{RhB} \cdot C_{RhB}} \quad (2)$$

where the K_{CV} and K_{RhB} are the adsorption constant on G-SERS substrate of CV, C_{CV} and C_{RhB} are the concentration of CV and RhB in solution respectively. According to Eq. (1), the surface coverage (θ) of CV and RhB can be calculated. $I_{m,CV}$ is the Raman intensity of CV molecules after saturated adsorption, which corresponding to the value at plateau region in Fig. S2. It was noted that when χ_{CV} was only 0.1 in the solution, the Raman intensity of CV was already comparable to that of RhB. When χ_{CV} reached 0.5, the spectral intensity was almost dominated by CV. This is a result of a few factors: the adsorption constants, the surface coverages and the Raman scattering cross sections. Fig. 3c shows the coverage dependence of CV and RhB calculated from the experiment data (dot data), which shows good correlation to the calculated result according to Eq. (2) (dash lines).

With the knowledge of adsorption constants and Raman scattering cross sections of CV and RhB, we mimicked the quantification of CV in a mixture solution with RhB using G-SERS. Fig. 4a shows the Raman spectra of CV of different concentrations in pure water. The relative intensities were plotted in the range from 10^{-8} M to 10^{-5} M, as the shown in Fig. 4c (blue line), and fitted using the single component Langmuir isothermal adsorption model [33]:

$$\frac{C_{CV}}{I_e} = \frac{C_{CV}}{I_{max}} + \frac{1}{I_{max} \cdot K_{CV}} \quad (3)$$

where C_{CV} is the concentration of CV molecules in solution, K_{CV} is the adsorption constant of CV on substrate, I_{max} and I_e represent the maximum Raman intensity in the plateau region and the measured Raman intensity at concentration C, respectively. The fitting coefficient of determination R^2 is as high as 0.998. However, when there is RhB existing in the solution, the curve deviated clearly, and the deviation depended on the concentration of RhB as shown in Fig. 4c. The corresponding Raman spectra of different concentration of pure CV and with 4×10^{-6} M RhB in solution were shown in Fig. 4a and b. The Raman intensity of CV follows Eq. (2) as depicted above. As the value of K_{RhB} (Fig. S3) and the concentration of RhB are known, thus $K_{RhB} \cdot C_{RhB}$ is a constant in the denominator. Eq. (2) was then used to fit the data in Fig. 4c, where a nice fitting is shown ($R^2 = 0.997$). From Eq. (2), it is seen that with a concentration of RhB, I_{CV} decreases more rapidly with the increase of C_{CV}, and the deviation is more significant with increasing C_{RhB}.

Fig. 5 shows the G-SERS spectra of CV (10^{-7} M), RhB (4×10^{-6} M) and their mixture, respectively. As depicted in Eq. (2), the Raman

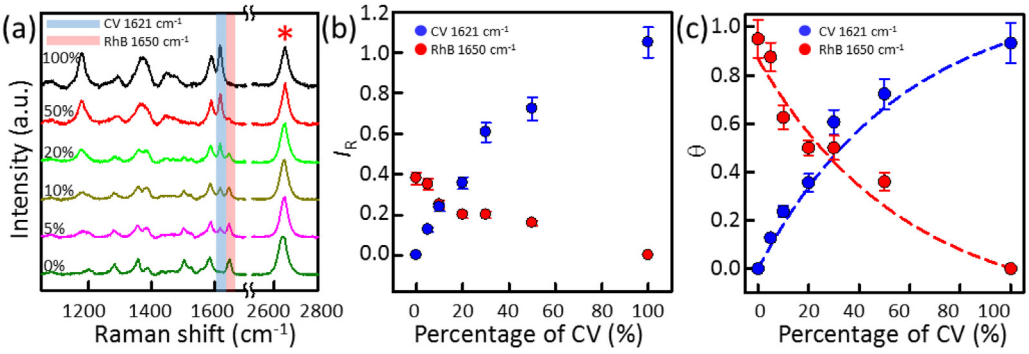

Fig. 3. (a) Raman spectra of mixed system of CV and RhB molecules with total concentration of 5×10^{-6} M in aqueous solution measured with G-SERS substrate. (b) Related Raman density (I_R), and (c) surface coverage of CV (peak 1621 cm^{-1}) and RhB (peak 1650 cm^{-1}) compared with graphene (peak 2650 cm^{-1}) as internal standard under different ratio of two components in solution.

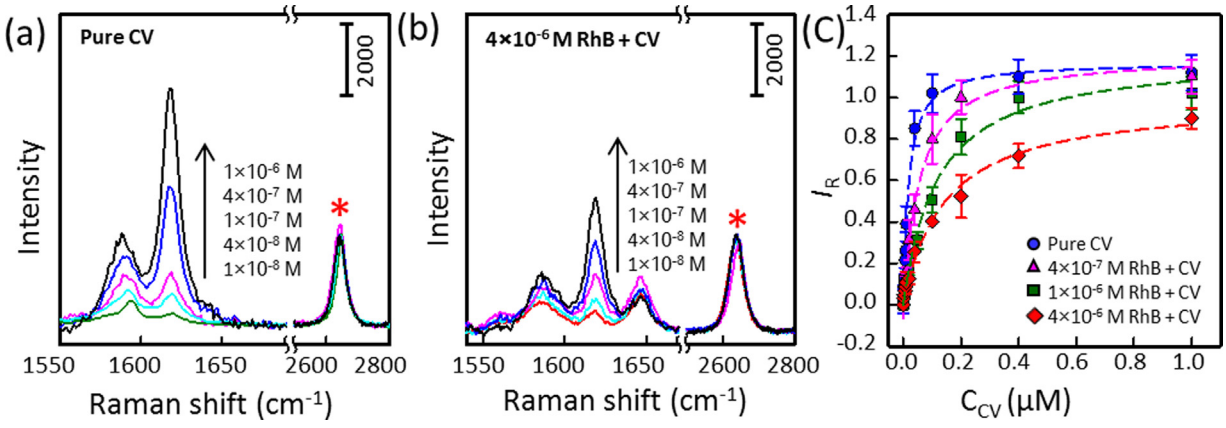

Fig. 4. Raman spectra of (a) pure crystal violet (CV) with different concentrations, and (b) when there is 4×10^{-6} M RhB molecule exist in the solution respectively. The concentration of CV in samples from bottom to up in (a and b) are as labeled; (c) the quantitative curve of pure CV, and when there is RhB exist in the solution with concentration of 4×10^{-7} M (pink line), 10^{-6} M (green line), and 4×10^{-6} M (red line) respectively. The dash lines are the fitting of experimental results using Eq. (2).

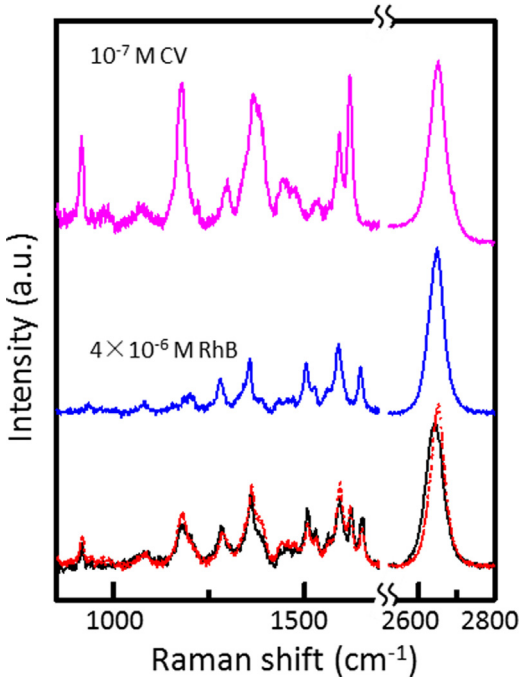

Fig. 5. G-SERS spectra of CV (10^{-7} M CV, red curve), RhB (4×10^{-6} M RhB, blue curve) and the mixture of 10^{-7} M CV and 4×10^{-6} M RhB. The black and red dash curves are the experimental and calculated SERS spectra, respectively.

spectrum of the mixture can be calculated by the value of binding constant (K_T), concentration (C), and $I_{m,i}$ of the two components:

$$I = \frac{I_{m,CV} \cdot K_{CV} \cdot C_{CV} + I_{m,RhB} \cdot K_{RhB} \cdot C_{RhB}}{1 + K_{CV} \cdot C_{CV} + K_{RhB} \cdot C_{RhB}} \quad (4)$$

From the red curve in Fig. 5, it is seen that the calculated result using Eq. (4) can well fit the experimental spectrum (black spectrum). According to Eq. (4), the value of $K_{CV} \cdot C_{CV}$ and $K_{RhB} \cdot C_{RhB}$ were known value, thus the value of $I_{m,CV}$ and $I_{m,RhB}$ can be calculated by knowing the integral Raman intensity of two components in the experiment data shown in Fig. 5 (black line). The value of $I_{m,CV}$ is ~4.3 times of $I_{m,RhB}$, which is consist with the slope of intensity vs. coverage (θ) as shown in Fig. S1. After normalized with the molecular size of the two molecules (1.95 nm^2 and 1.87 nm^2 respectively), the contribution of Raman intensity by each CV molecules is ~4.5 time larger than RhB, which reflects the ratio of Raman scattering cross section of two molecules on the surface of graphene. Ru et al. [5] reported that the intrinsic Raman scattering cross sections of CV (1621 cm^{-1}) and RhB (1652 cm^{-1}) under 633 nm excitation were 3.6×10^{-26} cm^2 sr^{-1} and 1.0×10^{-27} cm^2 sr^{-1}, respectively, meaning that the Raman scattering cross-section of CV is ~36 times to that of RhB. The difference of Raman scattering cross-section ratio of CV and RhB in aqueous and on G-SERS substrate means that the G-SERS substrate has different Raman enhancement factors for CV and RhB molecules, mainly owing to the different chemical enhancement, that is, the difference in molecular energy band alignments of CV and RhB to the Fermi level of graphene.

From above studies, we can see the value of K_{RhB} is also a key factor in deciding the influence of the interference molecules. Here

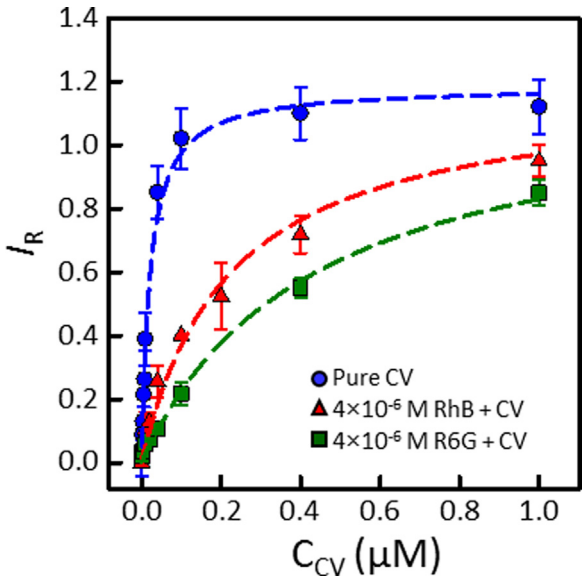

Fig. 6. The quantitative curve of CV without (blue line) and with exist of 4×10^{-6} M RhB (red line) and 4×10^{-6} M R6G (green line) respectively.

we chose another molecule Rhodamine 6G (R6G) which has similar structure but different adsorption constant with RhB as the interference molecules. Fig. 6 shows the quantitative curve of CV when there is RhB or R6G exist in the solution respectively. We can see that even the concentrations of RhB and R6G are both 4×10^{-6} M, the Raman intensities of CV are quite different. This results come from the different binding constant (K_T) of RhB and R6G molecules on graphene surface, thus the value of $K_{RhB} \cdot C_{RhB}$ and $K_{R6G} \cdot C_{R6G}$ are different. By fitting the experiment data with Eq. (4) that replace K_{RhB} and C_{RhB} with K_{R6G} and C_{R6G}, we can get the see that the binding constant of R6G was calculated to be $\sim 4.2 \times 10^6$ M^{-1}, which is about 3 time of K_{RhB}. Under the same concentration, the molecule with higher binding constant result in higher occupancy of surface coverage per unit of graphene area, leading to larger deviation than RhB.

From the above results, it can be found that the two factors determining the interference of one component with another in the binary system are the binding constant K_T and the concentration (C). These two factor together determine the coverage of the molecules occupy on graphene surface. When the value of $K_T \cdot C$ value is high, the competitive adsorption of interfering molecules on graphene surface is severe. In this case, the detected value of the target analyte deviates from the value determined from the quantitative curve of single component system. For component A in a solution with multiple components, Eq. (2) can be extended to:

$$I_A = \frac{I_{m,A} \cdot K_A \cdot (C_0 + C_A)}{1 + K_A \cdot (C_0 + C_A) + \sum K_i \cdot C_i} \quad (5)$$

where I_A is the Raman intensity of component A, K_A, C_0 and C_A are the binding constant, the unknown concentration and the known concentration of target component A, respectively. K_i and C_i are the binding constant and the concentration of component i in the solution. The standard curve can be obtained by adding in a series of known concentration of component A (C_A) in the solution. $\sum k_i \cdot c_i$ is the interference term for all components in solution which competitively adsorb on graphene surface with target molecules. The values of $\sum k_i \cdot c_i$ and $I_{m,A} \cdot K_A \cdot C_0$ are fixed, which can be obtained from the fitting result according to Eq. (5). From the fitted value of $I_{m,A} \cdot K_A \cdot C_0$, one can get the value of C_0 with the known values of $I_{m,A}$ and K_A.

4. Conclusion

To summarize, we explored the possibility of quantitative analysis of species in a mixture of solution by using G-SERS. For the ideal Langmuir adsorption of small dyes on graphene surface, the extended Langmuir isothermal fitting was applied for binary or multiple components systems. It was found that the Raman spectra of a mixture solution of dyes can be fitted using the concentration, the binding constant (K_T), and the saturated intensities of each single species on the surface of graphene. The quantitative analysis of the target analyte can be determined by correcting the competitive adsorption of the interfering components on graphene surface. These findings could be helpful for quantitative analysis of target analyte in practical complex systems.

5. Data availability

The raw/processed data required to reproduce these findings cannot be shared at this time as the data also forms part of an ongoing study.

Acknowledgements

J. Zhang, L. Tong acknowledge the funding from NSFC (51432002, 51720105003, 21790052, 11374355 and 21573004), the Ministry of Science and Technology of China (2016YFA0200100 and 2015CB932403), and the Beijing Municipal Science and Technology Project (Z161100002116026). H. Tian acknowledges funding from China Postdoctoral Science Foundation (2016M590011). We thank H. Wang, B. Deng for their supply of Chemical Vapor Deposition (CVD) method grown monolayer graphene for this work.

Appendix A. Supplementary data

Supplementary data associated with this article can be found, in the online version, at doi:10.1016/j.apmt.2019.01.008.

References

[1] P.L. Stiles, J.A. Dieringer, N.C. Shah, R.P. Van Duyne, Surface-enhanced Raman spectroscopy, Annu. Rev. Anal. Chem. 1 (2008) 601–626.
[2] J. Popp, T. Mayerhöfer, Surface-enhanced Raman spectroscopy, Anal. Bioanal. Chem. 394 (2009) 1717–1718.
[3] Z.Q. Tian, Surface-enhanced Raman spectroscopy: advancements and applications, J. Raman Spectrosc. 36 (2005) 466–470.
[4] D.Y. Wu, J.F. Li, B. Ren, Z.Q. Tian, Electrochemical surface-enhanced Raman spectroscopy of nanostructures, Chem. Soc. Rev. 37 (2008) 1025–1041.
[5] E.C. Le Ru, E. Blackie, M. Meyer, P.G. Etchegoin, Surface enhanced Raman scattering enhancement factors: a comprehensive study, J. Phys. Chem. C 111 (2007) 13794–13803.
[6] H.Y. Chen, M.H. Lin, C.Y. Wang, Y.M. Chang, S. Gwo, Large-scale hot spot engineering for quantitative SERS at the single-molecule scale, J. Am. Chem. Soc. 137 (2015) 13698–13705.
[7] A.B. Zrimsek, N.L. Wong, R.P. Van Duyne, Single molecule surface-enhanced Raman spectroscopy: a critical analysis of the bianalyte versus isotopologue proof, J. Phys. Chem. C. 120 (2016) 5133–5142.
[8] E.C. Le Ru, P.G. Etchegoin, Single-molecule surface-enhanced Raman spectroscopy, Annu. Rev. Phys. Chem. 63 (2012) 65–87.
[9] R.A. Alvarez-Puebla, L.M. Liz-Marzán, Traps and cages for universal SERS detection, Chem. Soc. Rev. 41 (2012) 43–51.
[10] S. Schlücker, Surface-enhanced Raman spectroscopy: concepts and chemical applications, Angew. Chem. Int. Ed. 53 (2014) 4756–4795.
[11] P. Wang, M. Xia, O. Liang, K. Sun, A.F. Cipriano, T. Schroeder, H. Liu, Y.H. Xie, Label-free SERS selective detection of dopamine and serotonin using graphene-Au nanopyramid heterostructure, Anal. Chem. 87 (2015) 10255–10261.
[12] H. Fang, X. Zhang, S.J. Zhang, L. Liu, Y.M. Zhao, H.J. Xu, Ultrasensitive and quantitative detection of paraquat on fruits skins via surface-enhanced Raman spectroscopy, Sens. Actuators B: Chem. 213 (2015) 452–456.
[13] S.E.J. Bell, N.M.S. Sirimuthu, Quantitative surface-enhanced Raman spectroscopy, Chem. Soc. Rev. 37 (2008) 1012–1024.

[14] W. Shen, X. Lin, C. Jiang, C. Li, H. Lin, J. Huang, S. Wang, G. Liu, X. Yan, Q. Zhong, B. Ren, Reliable quantitative SERS analysis facilitated by core–shell nanoparticles with embedded internal standards, Angew. Chem. Int. Ed. 54 (2015) 7308–7312.
[16] V. Peksa, M. Jahn, L. Štolcová, V. Schulz, J. Proška, M. Procházka, K. Weber, D. Cialla-May, J. Popp, Quantitative SERS analysis of azorubine (E 122) in sweet drinks, Anal. Chem. 87 (2015) 2840–2844.
[17] T. Nakabayashi, K. Kentaroh, N. Nobuyuki, Liquid structure of acetic acid studied by Raman spectroscopy and ab initio molecular orbital calculations, J. Phys. Chem. A 103 (1999) 8595–8603.
[18] H. Kang, S. Jeong, Y. Park, J. Yim, B.H. Jun, S. Kyeong, J.K. Yang, G. Kim, S. Hong, L.P. Lee, J.H. Kim, H.Y. Lee, D.H. Jeong, Y.S. Lee, Nanoprobes: near-infrared SERS nanoprobes with plasmonic Au/Ag hollow-shell assemblies for in vivo multiplex detection, Adv. Funct. Mater. 23 (2013) 3828.
[19] A. Kudelski, Raman studies of rhodamine 6G and crystal violet sub-monolayers on electrochemically roughened silver substrates: do dye molecules adsorb preferentially on highly SERS-active sites, Chem. Phys. Lett. 414 (2005) 271–275.
[20] S. Rieger, D. Grill, V. Gerke, C. Fallnich, Quantitative spontaneous Raman scattering spectroscopy in artificial binary lipid membranes, J. Raman Spectrosc. 48 (2017) 1264–1269.
[21] J.J. González-Vidal, R. Perez-Pueyo, M.J. Soneira, S. Ruiz-Moreno, Automatic identification system of Raman spectra in binary mixtures of pigments, J. Raman. Spectrosc. 43 (2012) 1707–1712.
[22] S.K. Srivastava, H.B. Hamo, A. Kushmaro, R.S. Marks, C. Grüner, B. Rauschenbache, I. Abdulhalim, Highly sensitive and specific detection of *E. coli* by a SERS nanobiosensor chip utilizing metallic nanosculptured thin films, Analyst 140 (2015) 3201–3209.
[23] Y. Zhang, P. Yang, M.A.H. Muhammed, S.K. Alsaiari, B. Moosa, A. Almalik, A. Kumar, E. Ringe, N.M. Khashab, Tunable and linker free nanogaps in core–shell plasmonic nanorods for selective and quantitative detection of circulating tumor cells by SERS, ACS Appl. Mater. Interfaces 9 (2017) 37597–37605.
[24] X. Qiao, B. Su, C. Liu, Q. Song, D. Luo, G. Mo, T. Wang, Selective surface enhanced Raman scattering for quantitative detection of lung cancer biomarkers in Superparticle@MOF structure, Adv. Mater. 30 (2018) 1702275.
[25] Y. Lu, J. Zhong, G. Yaoa, Q. Huang, A label-free SERS approach to quantitative and selective detection of mercury (II) based on DNA aptamer-modified SiO2@Au core/shell nanoparticles, Sens. Actuators B 258 (2018) 365–372.
[26] W. Xu, X. Ling, J. Xiao, M.S. Dresselhaus, J. Kong, H. Xu, Z. Liu, J. Zhang, Surface enhanced Raman spectroscopy on a flat graphene surface, Proc. Natl. Acad. Sci. U. S. A. 109 (2012) 9281–9286.
[27] H. Tian, N. Zhang, L. Tong, J. Zhang, In situ quantitative graphene-based surface-enhanced Raman spectroscopy, Small Methods 1 (2017) 1700126.
[28] L. Xie, X. Ling, Y. Fang, J. Zhang, Z. Liu, Graphene as a substrate to suppress fluorescence in resonance Raman spectroscopy, J. Am. Chem. Soc. 131 (2009) 9890–9891.
[29] W. Xu, N. Mao, J. Zhang, Graphene: a platform for surface-enhanced Raman spectroscopy, Small 9 (2013) 1206–1224.
[30] W. Xu, J. Xiao, Y. Chen, Y. Chen, X. Ling, J. Zhang, Graphene-veiled gold substrate for surface-enhanced Raman spectroscopy, Adv. Mater. 25 (2013) 928–933.
[31] I. Langmuir, The adsorption of gases on plane surfaces of glass, mica and platinum, J. Am. Chem. Soc. 40 (1918) 1361.
[32] J.A.V. Butler, C. Ockrent, Studies in electrocapillarity III, J. Phys. Chem. 34 (1930) 2841–2845.
[33] T. Liu, Y. Li, Q. Du, J. Sun, Y. Jiao, G. Yang, Z. Wang, Y. Xia, W. Zhang, K. Wang, H. Zhu, D. Wu, Adsorption of methylene blue from aqueous solution by graphene, Colloids Surf. B 90 (1) (2012) 197–203.